APL Materials

First proof-of-principle of inorganic perovskites clinical radiotherapy dosimeters

Cite as: APL Mater. **7**, 051101 (2019); https://doi.org/10.1063/1.5083810
Submitted: 30 November 2018 . Accepted: 02 April 2019 . Published Online: 03 May 2019

Mara Bruzzi, Cinzia Talamonti, Nicola Calisi, Stefano Caporali, and Anna Vinattieri

First proof-of-principle of inorganic perovskites clinical radiotherapy dosimeters

Cite as: APL Mater. 7, 051101 (2019); doi: 10.1063/1.5083810
Submitted: 30 November 2018 • Accepted: 2 April 2019 •
Published Online: 3 May 2019

Mara Bruzzi,[1,2] Cinzia Talamonti,[2,3,4] Nicola Calisi,[5] Stefano Caporali,[5] and Anna Vinattieri[1,2]

AFFILIATIONS

[1]Università degli Studi di Firenze, Dipartimento di Fisica ed Astronomia, Via G. Sansone 1, 50019 Sesto Fiorentino, Firenze, Italy
[2]Istituto Nazionale di Fisica Nucleare, Sezione di Firenze, Via G. Sansone 1, 50019 Sesto Fiorentino, Firenze, Italy
[3]Università degli Studi di Firenze, Dipartimento di Scienze Biomediche Sperimentali e Cliniche "Mario Serio," Viale Morgagni 50, 50133 Firenze, Italy
[4]Azienda Ospedaliero Universitaria Careggi, SOD Fisica Medica, Largo Brambilla 3, 50134 Firenze, Italy
[5]Università degli Studi di Firenze, Dipartimento di Ingegneria Industriale, Via S. Marta 3, 50139 Firenze, Italy

Note: This paper is part of the special topic on Perovskite Semiconductors for Next Generation Optoelectronic Applications.

ABSTRACT

Inorganic $CsPbBr_3$ perovskite devices have been manufactured and tested as dosimeters under both conventional and Intensity Modulated Radiotherapy (IMRT) X-ray beams. Samples showed a very good linear dependence of the collected charge/current on dose/dose rates in the range of 0.1–5.0 Gy/0.1–4.0 Gy/min of interest for clinical applications. A device sensitivity of about 70 nC/Gy mm^3 compares favorably with other solid-state dosimeters. The first verification of an IMRT dose profile of a prostate cancer treatment, performed by moving the perovskite device on a 10 cm-long profile with a 0.5 mm pitch, showed agreement within 5% with the dose distribution required by the treatment planning system.

I. INTRODUCTION

Modern radiotherapy techniques, such as X-photon Intensity Modulated RadioTherapy (IMRT) and Volumetric Modulated Arc Therapy (VMAT), deliver highly conformed doses to irregularly shaped tumor volumes to spare surrounding healthy tissues.[1,2] The consistency between dose maps calculated by a dedicated Treatment Planning System (TPS) and those actually delivered to the patient have to be carefully checked experimentally either before or during the patient treatment. Modern dosimetric systems need precise measurements of the dose map distributions, characterized by high spatial resolutions. For this purpose, the active volume of the dosimeter must be minimized; therefore, a material with high sensitivity per unit volume is required.

Solid-state dosimeters behave as ionization chambers during X-ray irradiation; electron-hole pairs are generated in the semiconductor bulk and then collected by the electric field applied across electrodes.[3] The charge Q collected at electrodes, in general, has a linear dependence on the absorbed dose, D, and sensitivity per unit volume is given by $S = \frac{Q}{D\,Volume} = \frac{qG}{R}$, with G being the electron-hole pair generation rate, R being the absorbed dose rate, and q being the electronic charge. The generation rate is related to the dose rate R by $G = \frac{R\rho}{E_i}$, with ρ being the density and E_i being the mean energy to create an electron-hole pair.[4] Thus, the sensitivity S per unit volume is ultimately ruled out by the ratio between density and mean energy for pair production: $S = \frac{q\rho}{E_i}$. State-of-art dosimeters for clinical radiotherapy are ionization chambers (ICs) filled with air, silicon diodes, and, more recently, also diamond films. As an example, Table I shows a list of relevant parameters for three radiotherapy dosimeters based on ICs,[5] Si diodes,[4,6] and single-crystal Chemical Vapor Deposited (CVD) diamond, respectively.[7] The first two are modular arrays developed specifically for IMRT applications, while the third is a pin-point device, a bidimensional device based on this material being still under development.[8]

In clinical radiotherapy, X-ray beams are characterized by high dose rates and high energy in the 0.05–18 Gy/min and MeV ranges, respectively, much higher than those used for X-ray inspection and

TABLE I. Relevant properties of commercial dosimetric devices used in clinical radiotherapy applications.

	IC (air)	Silicon	Diamond
ρ (g/cm^3)	1.29×10^{-3}	2.33	3.52
E_i (eV)	34.00	3.60	16.20
S (nC/Gy mm^3)	0.038	647.22	217.28
Area (mm^2)	25.00	0.64	3.80
Thickness (mm)	5.00	0.03	0.001
Volume (mm^3)	125	0.019	0.0038
Array	OCTAVIUS PTW	MAPCHECK SunNuclear	...
Detector	729 PTW	SunPoint® diode detector	MicroDiamond type 60019 PTW
Reference	5	6	7

imaging, where dose rates are of the order of few micrograys per second and energy is hundreds of keV. With dose-rates and energies typical of clinical radiotherapy, a volume of about 1 mm^3 or less is sufficient to get currents of the order of 1 nA from a semiconductor device, this brings to adopting active layers of small thickness (not in the case of ionization chambers, where the low density of air needs for higher volume and depth). Moreover, a thick slab of a semiconductor material would suffer from a reduction in sensitivity with the accumulated dose due to the diffusion length decrease caused by radiation-induced defects.[9] In fact, commercial silicon and diamond devices are characterized by a thickness of the order of 1–30 μm (see Table I).

In $CsPbBr_3$, the mean energy to create an electron-hole pair has been estimated as $E_{CsPbBr_3} \sim 5.3$ eV[10] by extrapolating results from a class of compound materials used in X-ray detection.[11] Considering $\rho_{CsPbBr_3} = 4.55$ g/cm^3, one obtains a theoretical value $s_{CsPbBr_3} \sim 860 \frac{nC}{Gy\,mm^3}$, much higher than that of silicon and far above that of diamond. This material is even more favorable than $MAPbBr_3$: in fact, given $\rho_{MAPbBr3} = 3.83$ g/cm^3[12] and $E_{MAPbBr_3} = 6.03$ eV,[13] one obtains a theoretical value $s_{MAPbBr_3} \sim 635 \frac{nC}{Gy\,mm^3}$, lower than that of $CsPbBr_3$. $CsPbBr_3$ has already been proposed as an X-ray photodetector and imaging device in medical applications,[14–17] but up to now, no work has been carried out to demonstrate the feasibility of using this material to produce and test photoconductive dosimeters for clinical radiotherapy. Moreover, there is a second important reason that makes it extremely interesting to develop $CsPbBr_3$ dosimeters for clinical radiotherapy. Modern systems involve three-dimensional geometries, often based on nonplanar arrangements, e.g., cylindrical water-equivalent phantoms equipped with three-dimensional arrays of detectors placed in a helicoidal pattern.[18] Solid-state semiconductor devices, such as silicon diodes and diamond Schottky barriers, are manufactured from semiconductor wafers, rigid and with flat geometry, not suitable for nonplanar geometry arrangements. $CsPbBr_3$ inorganic perovskites can be in principle easily deposited on flexible large area supports to create a multipoint device adjustable on any kind of shape. This adding value of $CsPbBr_3$ makes this material a very promising candidate for modern clinical dosimetry applications.

In this work, we present a first proof-of-principle experimental study on the feasibility of $CsPbBr_3$ dosimeters for clinical radiotherapy, with particular focus to IMRT modality. We manufactured a set of point devices by depositing thin films on custom printed circuit boards (PCB) equipped with electrodes and tested them under clinical X-ray beams used in advanced radiotherapy accelerators, in view to develop advanced dosimetric systems for modern clinical radiotherapy.

II. EXPERIMENTAL PROCEDURE

$CsPbBr_3$ films have been deposited by drop-cast directly on alumina Printed Circuit Board (PCB) specially designed for electrical tests of thin semiconductor films. The perovskite film is obtained starting from CsBr and $PbBr_2$ salts (Acros Organics, >99%) mole ratio 1:1 in a dimethyl sulfoxide (DMSO, from Sigma-Aldrich) saturated solution. Thermal annealing at 150 °C eliminates traces of the solvent and returns a layer of interconnected $CsPbBr_3$ microcrystals of the order of a few micrometer. The alumina PCBs have two parallel gold contacts, 7 mm long and spaced 0.8 mm, 20 μm thickness. Figure 1(a) shows a picture of one of the devices tested in this study in X-ray diffraction inspection, shown in Fig. 1(b), together with XPS analysis, demonstrated the excellent quality of the film in the absence of residual precursors and contaminants. Figure 1(c) shows an SEM photograph evidencing the microcrystalline nature of the film. Low temperature (10 K) photoluminescence analysis [Fig. 1(d)] carried out on a similar drop-casted sample deposited on a glass substrate evidenced high-quality emission properties, similar to the literature data.[19] Soon after deposition, we covered the perovskite film with a polymethylmethacrylate (PMMA) layer to prevent degradation due to air and moisture contact and to favor electronic equilibrium during the exposure to therapeutic X-ray beams.

A recent study on the photoconductive properties of similar samples showed a resistivity in the dark about 10^9 Ω cm and a positive value of the Hall coefficient $R_H \sim 10^{10}$ cm^3/C, indicating p-type conductivity with a Hall mobility $\mu_H = R_H/(r_H\rho) \sim 10$ cm^2/(Vs).[20] We tested the dosimetric properties of our devices with clinical X-ray beams delivered by linear accelerators (LINAC) routinely used for patient treatments at the Radiotherapy Unit of the University Hospital in Florence. A Precise Elekta linac delivering 6 MV and 25 MV X-ray beams (meaning that X-ray highest energy is 6 MeV

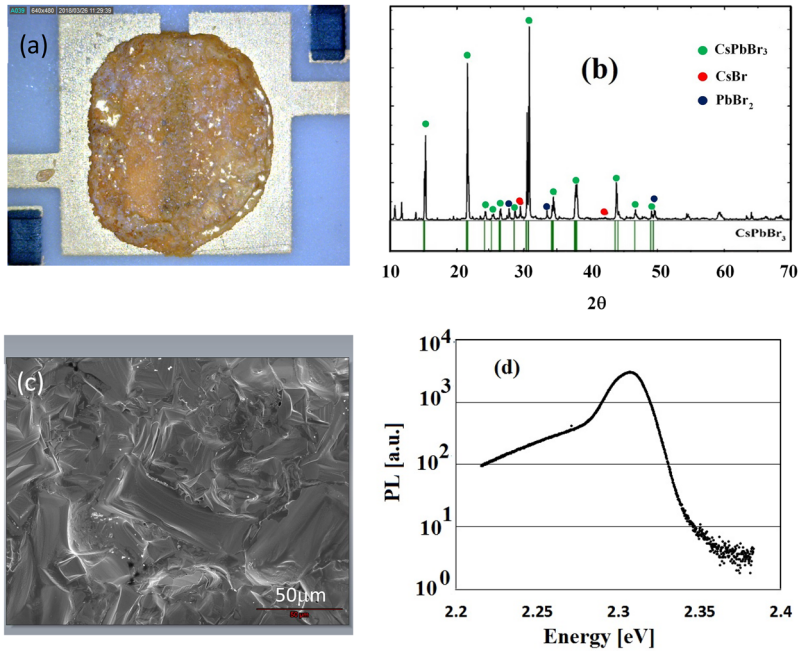

FIG. 1. (a) Photograph of the $CsPbBr_3$ film deposited on the alumina substrate carrying two parallel gold contacts, (b) XRD spectrum of the film, (c) SEM image showing the microcrystalline nature of the deposit, and (d) photoluminescence spectrum of a similar drop-casted sample deposited on a glass substrate.

and 25 MeV, respectively), in the nominal dose rate range of 0.5–4 Gy/min, was used. The linac dose rate was checked during the tests using the ionization chambers placed within the linac; it is stable within 0.01 Gy/min. Each perovskite-based device has been placed at the isocenter, namely, at Source Axis Distance (SAD) = 100 cm, corresponding to Source Skin Distance SSD = 95 cm, beyond a 5 cm-thick polymethylmethacrylate layer to ensure electronic equilibrium during irradiation. A first test has been carried out with a uniform squared field of irradiation (40 × 40 cm^2) and linac gantry at an angle of 0° to determine the sensitivity of our devices to doses and dose/rates typically used in clinical radiotherapy. Current flowing across the two electrodes, biased with a constant voltage of 5 V, was read out by a Keithley 6517 electrometer (also used as a voltage source) driven by a Matlab software toolkit. The current response has been read out during irradiation; the device has been tested under doses (0.1–5.0 Gy) and dose rates (50–400 cGy/min) of interest in clinical radiotherapy. A moderate drift of the current stabilized itself after the first minutes of voltage application. The device is also sensitive to local temperature changes, which can occur during irradiation and give rise to fluctuations in the baseline due to the dark current, which is anyway subtracted from the photocurrent signal.

A second test has been carried out to investigate the performance of our perovskite-based dosimeter in a high conformal radiotherapy technique such as IMRT (Intensity Modulated Radio-Therapy). An Elekta Synergy linac equipped with a Multi-Leaf Collimator (MLC) composed of 80 4 mm-thick leaves has been used to deliver a clinical 10 MV photon beam out of five planned for an IMRT prostate treatment. The IMRT treatment was delivered in the step-and-shoot modality which means that dose is released during a discrete set of irradiation steps, each characterized by a selected configuration of the MLC, in view to have a suitable aperture shape at the linac head (segment), irradiating only when leaves are stationary at each position. The dose bidimensional map is obtained by summing 12 successive segments, with gantry placed at 0°, carried out with a nominal dose rate of 400 cGy/min, each with a different spatial distribution. Each segment has a duration of a few seconds; the entire radiation treatment lasts about 1 min. Figure 2 shows the TPS IMRT dose map of the beam used in this work. We tested our

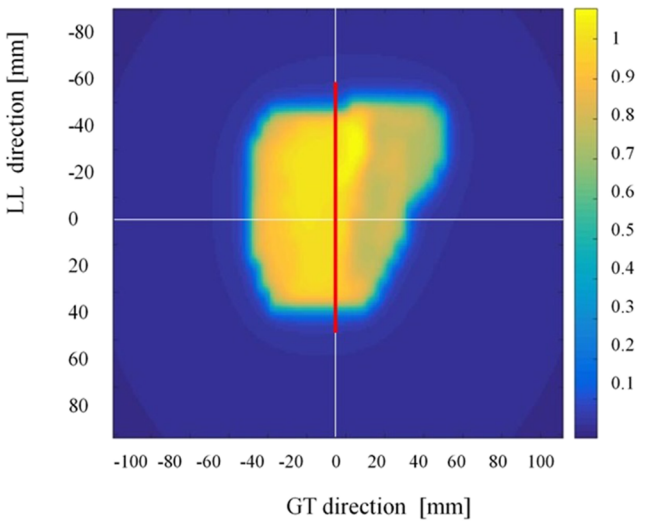

FIG. 2. TPS map of doses, typical of a prostate cancer treatment used in this study: GT = gantry target direction and LL = lateral–lateral direction (isocenter at the intersection of the white lines). The solid red line indicates the profile studied in this work.

device acquiring data along a lateral-lateral profile passing through the isocenter (shown in Fig. 2) by changing its position from bottom to top with 5 mm-pitch, for a total elongation of 10 cm. We measured the current during each segment, and we calculated the total collected charge by integrating the overall signal during time, after subtracting the baseline due to dark current. Baseline fluctuations during measurement are lower than 1% of the signal.

III. EXPERIMENTAL RESULTS

Figure 3(a) shows the photocurrent (after the dark current subtraction) measured by our device when biased with 5 V and irradiated by a 25 MV X-ray beam with pulses of increased duration. Each pulse, delivered with the same dose rate (200 cGy/min), refers to a different dose value in the range of 0.1–5 Gy of interest in clinical radiotherapy. Figure 3(b) shows the collected charge obtained by integrating such current signals, plotted as a function of the dose. The best fit of data evidences an excellent linear trend, indicating a constant sensitivity in the overall investigated range, even in the low dose range, with very short pulses. Figure 3(c) shows a comparison of the current signals measured up to 50 cGy: signal transients are rather slow but well reproducible at any investigated duration. A very good linear trend in the whole charge vs dose investigated range is obtained (see the inset), characterized by the same slope and almost the equal intercept.

We calculated the sensitivity of our device to dose as the slope of the linear plot of charge vs dose shown in Fig. 3(b), $S = \frac{Q}{D} = 7.82\ \frac{\text{nC}}{\text{Gy}}$, considering the geometry of this device, a sensitivity per unit volume: $s = 69.8\ \frac{\text{nC}}{\text{Gy mm}^3}$ is obtained. The intercept of the curve, $q = 48.5pC$, can be considered as the resolution in charge of our device, corresponding to about 6.2 mGy. The dose-rate dependence of the current response of our perovskite device has been investigated with another sample under a 6 MV X beam in the range of 0.5–4 Gy/min of interest in clinical radiotherapy. Current signals are shown in Fig. 4(a); the average current measured at signal saturation at each dose rate is plotted against the dose rate in Fig. 4(b).

The sensitivity of our device, in this case, is $S_{Dr} = \frac{\Delta I}{D_r} = 5.9\frac{\text{nC}}{\text{Gy}}$. Considering the geometry of this sample, the sensitivity per unit

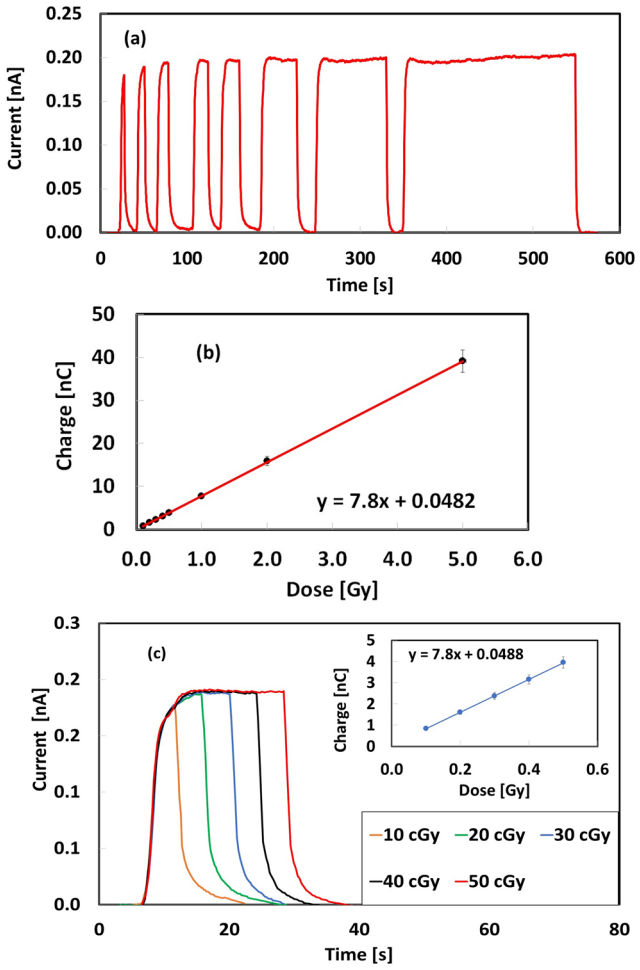

FIG. 3. (a) Current signal as a function of time measured during repeated pulses of different duration with the $CsPbBr_3$ film (5 V bias) under an X-ray beam with the 25 MeV highest energy. (b) Charge obtained by integrating current signals shown in (a), plotted as a function of the dose with a linear best fit. (c) Comparison of current signals measured in the low dose range of 10–50 cGy, linear behavior of the charge vs dose in the same range.

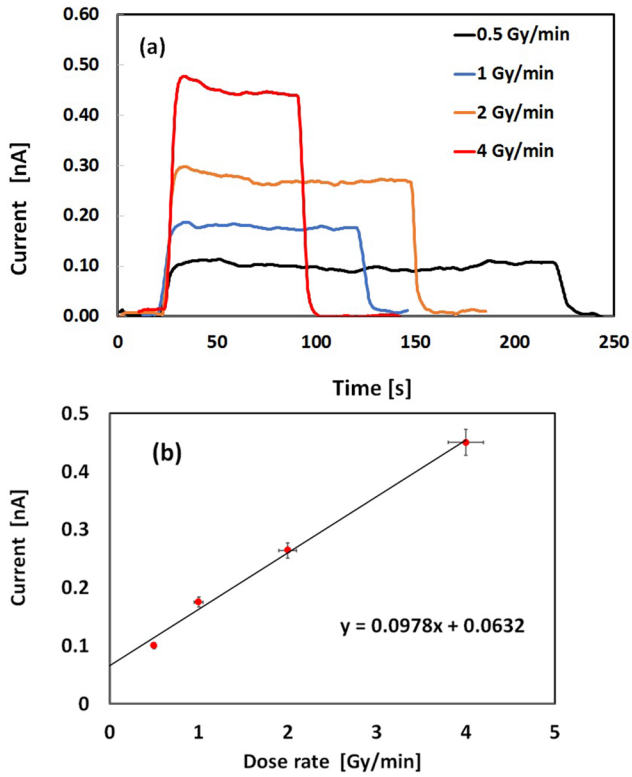

FIG. 4. (a) Current signal measured with a $CsPbBr_3$ dosimeter (V_{bias} = 5 V) when irradiated under 6 MV X-rays with four different dose rates and same total dose (2 Gy) and (b) current signal measured at saturation plotted as a function of the dose rate and best-fit showing a linear behavior.

volume is $s = 70.5 \frac{\text{nC}}{\text{Gy mm}^3}$, in good agreement with results obtained when charge vs dose and a 6 MV X beam has been used.

The good linear dependence against dose and dose rate, as well as stable and reproducible responses measured under conventional uniform radiation fields, is a promising feature for achieving good results also in high conformal radiation modality such as intensity modulated radiotherapy (IMRT). We carried out the first investigation under an IMRT field, as described in Sec. II. We show results in Figs. 5(a) and 5(b). Twelve irradiation segments are clearly visible in the plots as separated current/charge signals, indicating that our device can follow the fast and complex structure of this high conformal radiotherapy technique. Dose profile relative to isocenter, measured with the perovskite-based dosimeter by moving it on a 10 cm along a line (shown in Fig. 2) with a 5 mm pitch, is shown in Fig. 5(c). It is compared to the same profile given by the treatment planning system and by a commercial dosimetric system made of a flat silicon diode bidimensional array (MAPCHECK^{TM} by Sun Nuclear Corporation Melbourne, FL, USA).[6] Our data are in very good agreement, within 5% error, with the profile required by the TPS software and measured the reference dosimetric system. This experimental test is a valid proof that a perovskite-based device is indeed able to follow the complex radiation delivering used in an IMRT technique and opens the way to the application of inorganic perovskite dosimeters for modern radiotherapy in conformal modality.

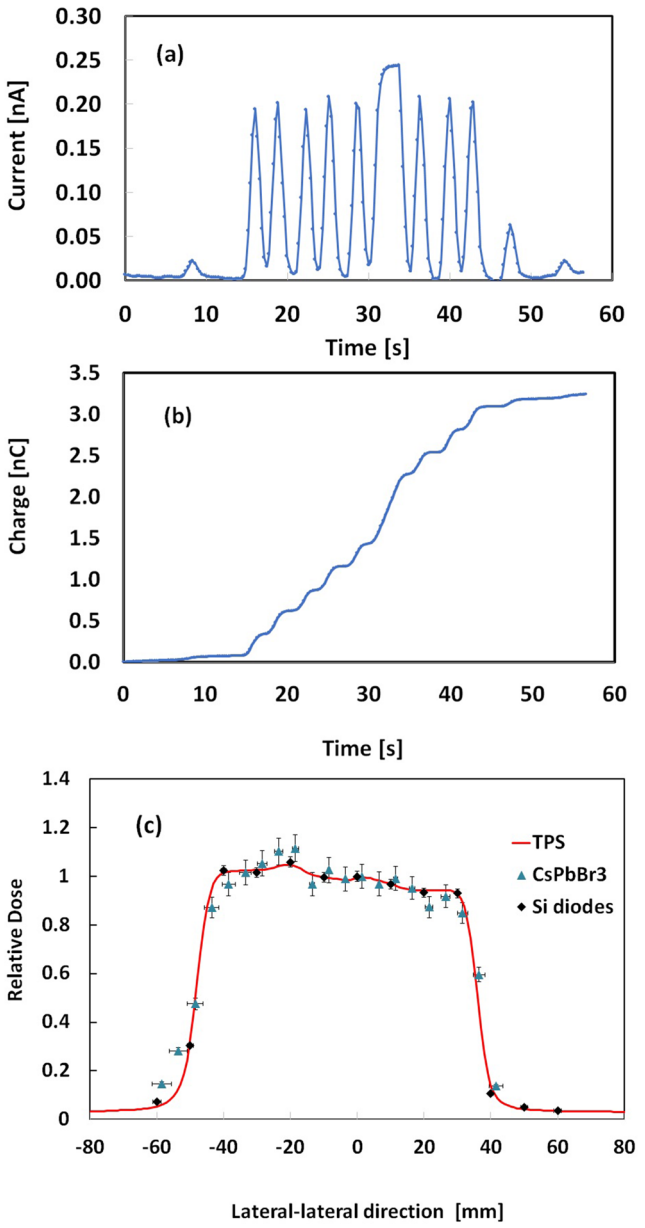

FIG. 5. (a) Current and (b) charge signals measured with the perovskite dosimeter under the IMRT beam (bias 5 V) of the TPS map shown in Fig. 2. (c) Dose profile, relative to isocenter, measured with the perovskite-based dosimeter and with an array of commercial Si diodes (MAPCHECK by Sun Nuclear Corporation Melbourne, FL, USA) as compared to the same profile obtained from the treatment planning system.

IV. CONCLUSIONS

A set of inorganic $CsPbBr_3$ perovskite microcrystalline films have been deposited on custom printed circuit boards (PCBs) and tested as dosimeters with therapeutic X-ray beams. Current/charge signals are linear with dose/dose rates under 6 MV/25 MV X-ray uniform irradiation fields from linac, within dose and dose rate ranges 0.1–5 Gy, 0.1–4 Gy/min of interest for clinical applications. The sensitivity per unit volume found in our samples is about 70 nC/Gy mm^3; the lowest measurable dose is about 6 mGy, far below the machine lower delivering limit (1 cGy). The sensitivity per unit volume calculated by our devices is smaller than the theoretical value estimated for $CsPbBr_3$. This is probably due to recombination at defects. Acting as a sink of electrons and holes, they reduce the charge collected at electrodes. As a result, the effective distance each electron-hole pair travel apart before being recombined (so-called effective charge collection length) is lower than the total thickness. The effective active volume of the device is thus reduced to a fraction of the entire volume of the sample. A recent study carried out by some of the authors on similar samples pointed out that in such a microcrystalline material, a non-negligible concentration of defects, probably located at grain boundaries of the microcrystals involved in the photoconductivity response of the devices at room temperature.[20] We note that this effect is also found in polycrystalline diamond dosimeters, e.g., in Ref. 21, where a device with an active area 1.8 × 18 mm^2 and a thickness of 300 μm, biased with 5 V, showed under a 6 MV X-ray beam of 38 nC/Gy sensitivity, indicating a charge collection length of about 55 μm, significantly lower than the total thickness of the sample. In silicon dosimeters, instead, problems are related to the formation of radiation-induced defects, which degrades the diffusion length and causes changes in the sensitivity with the accumulated dose. To overcome this problem, the thickness of the active volume, in most commercial devices, is tailored opportunely to values around 20–50 μm.[9] Hence, even if the sensitivity per unit volume of silicon is quite higher, the actual sensitivity of the device has a similar constraint found for diamond and perovskite samples.

A first study in high conformal irradiation modality has also been performed using an intensity modulated radiotherapy (IMRT)

beam. A conformal dose distribution planned for prostate cancer treatment has been verified by measuring the current signal of the perovskite device at several points within the irradiation field map, along with a 10 cm-long profile passing through the isocenter, with a 0.5 mm pitch. Our data showed a good agreement with the dose distribution required by the treatment planning system, with errors within 5%, indicating that our $CsPbBr_3$ perovskite dosimeters can actually meet the stringent requirements of modern clinical radiotherapy techniques.

In forthcoming studies, we plan to study the dosimetric performance of single crystal inorganic perovskite samples, in view to increase the sensitivity of our devices toward the theoretical limit. In addition, we wish to investigate the effect of radiation-induced defects on sensitivity, both for polycrystalline and single crystal $CsPbBr_3$, to finally assess the possible application of these materials in radiotherapy.

ACKNOWLEDGMENTS

Work performed under the framework of the project: advanced optical spectroscopy for interface control in perovskite-based solar cells, funded by Fondazione CARIFI Bando 2017.

REFERENCES

[1] S. Webb, Lancet Oncol. **1**(1), 30 (2000).
[2] R. Allison, C. Sibata, and R. Patel, Future Oncol. **9**(4), 493 (2013).
[3] M. Bruzzi, Nucl. Instrum. Methods Phys. Res., Sect. A **809**, 105 (2016).
[4] C. A. Klein, J. Appl. Phys. **39**, 2029 (1968).
[5] See https://www.ptw.de/3097.html for OCTAVIUS detector 729, PTW, Freiburg, Germany.
[6] See https://www.sunnuclear.com/documents/datasheets/arccheck3dvh.pdf for an example of state-of-art silicon diodes array in volumetric quality assurance measurements.
[7] See https://www.ptw.de/2733.html for Synthetic diamond detector, microDiamond type 60019, PTW, Freiburg, Germany.
[8] M. Scaringella, M. Zani, A. Baldi, M. Bucciolini, E. Pace, A. de Sio, C. Talamonti, and M. Bruzzi, Nucl. Instrum. Methods Phys. Res., Sect. A **796**, 89 (2015).
[9] M. Bruzzi, M. Bucciolini, M. Casati, D. Menichelli, and C. Talamonti, Appl. Phys. Lett. **90**, 172109 (2007).
[10] Y. He, L. Matei, H. J. Jung, K. M. McCall, M. Chen, C. C. Stoumpos, Z. Liu, J. A. Peters, D. Y. Chung, B. W. Wessels, M. R. Wasielewski, V. P. Dravid, A. Burger, and M. G. Kanatzidis, Nat. Commun. **9**, 1609 (2018).
[11] A. Owens and A. Peacock, Nucl. Instrum. Methods Phys. Res., Sect. A **531**, 18 (2004).
[12] D. Weber, "$CH_3NH_3PbX_3$, a Pb(II)-system with cubic perovskite structure," Z. Naturforsch., B: J. Chem. Sci. **33**, 1443–1445 (1978).
[13] H. Wei, Y. Fang, P. Mulligan, W. Chuirazzi, H.-H. Fang, C. Wang, B. R. Ecker, Y. Gao, M. A. Loi, L. Cao, and J. Huang, Nat. Photonics **10**, 333 (2016).
[14] Y. Lee, J. Kwon, E. Hwang, C. H. Ra, and W. J. Yoo, Adv. Mater. **27**, 41 (2015).
[15] J. A. Rowlands, Nature **550**, 47 (2017).
[16] H. S. Gill, Phys. Med. **5**, 20 (2018).
[17] W. Wei, Y. Zhang, Q. Xu, H. Wei, Y. Fang, Q. Wang, Y. Deng, T. Li, A. Gruverman, L. Cao, and J. Huang, Nat. Photonics **11**, 315 (2017).
[18] G. Li, Y. Zhang, X. Jiang, S. Bai, G. Peng, K. Wu, and Q. Jiang, Phys. Med. **29**(3), 295 (2013).
[19] X. Li, F. C. D. Yu, J. Chen, Z. Sun, Y. Shen, Y. Zhu, L. Wang, Y. Wei, Y. Wu, and H. Zeng, "All inorganic halide perovskites nanosystem: Synthesis, structural features," Opt. Prop. Optoelectron. Appl. **13**(9), 1603996 (2017).
[20] M. Bruzzi, F. Gabelloni, N. Calisi, S. Caporali, and A. Vinattieri, Nanomaterials **9**, 177 (2019).
[21] M. Zani, M. Bucciolini, A. De Sio, R. Mori, E. Pace, M. Scaringella, C. Talamonti, L. Tozzetti, and M. Bruzzi, Nucl. Instrum. Methods Phys. Res., Sect. A **730**, 129 (2013).